UCRL- 88313
PREPRINT
Conf-821128--4

Studying Electron Distributions Using the Time-Resolved Free-Bound Spectra From Coronal Plasmas

D. L. Matthews
R. L. Kauffman

J. D. Kilkenney
R. W. Lee

American Physical Society 24th Annual Meeting
New Orleans, LA
November 1-5, 1982

November, 1982

Lawrence Livermore National Laboratory

Studying Electron Distributions Using the Time-Resolved Free-Bound Spectra From Coronal Plasmas*

UCRL--88313

DE83 006569

D. L. Matthews, R. L. Kauffman

Lawrence Livermore National Laboratory

and

J. D. Kilkenny, R. W. Lee

Imperial College, London, England

Abstract

Absorption of laser light in a plasma by inverse bremsstrahlung, I.B., can lead to a non-Maxwellian velocity distribution provided the electron-electron collision frequency is too low to equilibrate the velocity distribution produced by I.B. We study the electron distribution in the coronal plasma region of a laser heated aluminum disk by measuring the radiation recombination continuum. The experiments are performed using $\lambda_L = 0.532$ μm laser light at intensities of $\sim 10^{16}$ W/cm^2. Such parameters are predicted to produce conditions suitable for a non-thermal electron distribution. The shape of the K-shell recombination radiation has been measured using a time-resolved x-ray spectrograph. The electron distribution can be determined from deconvolution of the recombination continuum shape.

*Work performed under the auspices of the U.S. Department of Energy by Lawrence Livermore National Laboratory under contract #W-7405-ENG-48.

Introduction

Laser light absorption[1,2,3] by inverse bremsstrahlung remains an important process by which energy can be efficiently delivered to inertial confinement fusion targets. Light absorption by other physical processes such as resonance absorption[4,5] or ion-acoustic turbulence[3,6,7] are also important but can lead to production of high energy electrons which preheat and therefore degrade the performance of an ablative implosion. The trend in present day fusion targets is toward higher Z plasmas produced by low laser intensities, short laser wavelengths and long laser pulses. These conditions are of course optimum for absorption by inverse bremsstrahlung. However for materials with $Z \gg 1$ and at even moderate laser intensities, absorption by inverse bremsstrahlung is expected to be reduced due to non-linear effects. In fact, Langdon[1] has calculated that when $Z(v_0/v_t)^2 \geq 1$, inverse bremsstrahlung results in a non-Maxwellian velocity distribution weighted toward higher electron energies than are optimum for the absorption process. In this work we investigate the electron distribution by measuring the energy spectrum of aluminum K-shell recombination radiation. We demonstrate that the shape of the recombination spectra can be used to determine the electron distribution function. To optimize absorption by inverse bremsstrahlung, the experiments are performed with green light (λ_L = 0.532 μm) and with fairly long pulselengths ($\tau_L \sim$ 900 psec). The $Z(v_0/v_t)^2 \geq 1$ criterion is predicted to be satisfied by performing the experiments with aluminum (Z = 13) and $I_L \sim 10^{16}$ W/cm^2.

I. Definition of Experiment

Laser light absorption by inverse bremsstrahlung is due to classical electron-ion collisions. Langdon[1] demonstrated that the time evolution of an initially monoenergetic electron distribution, v_0, under the perturbation of electron-ion collisions -- assuming $Z \gg 1$ and neglecting $e^- - e^-$ collisions -- progresses towards a flat (or constant) distribution for $v_t < v_0$. Here, v_t is the electron thermal velocity $\left(\frac{KT}{m}\right)^{1/2}$ and v_0 is the electron "quiver" velocity -- corresponding to light absorption at an electron ion collision rate equal to the laser frequency. This phenomemon occurs if the electrons gain energy from the laser faster than they can thermalize (through $e^- - e^-$ collisions) or if

$$Z\left(\frac{e\,E_L}{m_e \omega_L v_t}\right)^2 > 1 \qquad (1)$$

where E_L is the laser energy and ω_L is the laser frequency.

In Figure 1 we show Langdon's results for the electron velocity distribution function, f(v), of a Maxwellian and a strong non-Maxwellian ($Z\,(v_0/v_t)^2 = 6$). For the measurements discussed here, $Z(v_0/v_t)^2 \sim 7$ since $(v_0/v_t)^2 = 4 \times 10^{-16}\, I\lambda^2/T_e$, where $I(W/cm^2)$, λ(microns), T_e(keV) assuming $Z = 13$ (fully ionized), $T_e \sim 1$ keV, $I \sim 0.5\text{-}1.0 \times 10^{16}$ W/cm^2 and $\lambda_L = 0.532$ μm.

The derivation of the emission rate for the free-bound continuum of a hydrogenic ion is obtained by noting that photoionization and radiative recombination are inverse processes, and are in detailed balance. Since we can derive the free-bound emission rate per ion and electron having velocity v, then the non Maxwellian (non-thermal) emission can be determined by using the appropriate non-Maxwellian distribution function.

First the absorption coefficient for frequency ν from hydrogenic ion in state n'

$$\alpha_\nu = \left(\frac{64\, e^{10}\, \pi\, m^4}{3\sqrt{3^6 h\, e}} \right) \left(\frac{1}{(n')^5\, \nu} \right) \tag{2}$$

Defining $F(v)$ as the probability of there being an electron with velocity v then we know that

$$n_I\, n_e\, (v)\, F(v)\, v\, dv\, dt \tag{3}$$

is the number of "recaptures" and ν is related to velocity by

$$h\nu = E_{IONIZATION} + 1/2\, mv^2\ , \tag{4}$$

i.e., by energy conservation. Therefore the emission per unit frequency per unit is

$$n_\nu = h\nu\, n_I n_e(v)\, F(v)\, v\, dv = \left(\frac{h^2 \nu}{m} \right) n_I n_e(v)\, F(v)\, dv \tag{5}$$

To relate $F(v)$ to the absorption cross-section α_ν of Eq. 2, we use the continuum analog of the Einstein-Milne relations and find

$$\alpha_\nu = \left(\frac{4\pi c^2 m^2 \nu^2}{h^2 \nu^2}\right)\left(\frac{g_1}{g_0}\right) \quad F(v) \tag{6}$$

here we use g_1, g_0 as the degeneracy of higher and lower ionization stage. Substitution leads to

$$\eta_\nu = Z^4 n_I n_e(v) \left(\frac{e^{10} 16 \pi^3}{3\sqrt{3}\, m^2 c^3 h^2}\right)\left(\frac{g_0}{g_1}\right)\left(\frac{1}{v^2}\right) \tag{7}$$

we thus have for the recombination continuum

$$\eta_\nu = \frac{n_e(v)}{v^2} \cdot A \tag{8}$$

where A contains the constants that do <u>not</u> depend on the velocity distribution. The emission can now be characterized by specifying the velocity distribution;

$$n_e(v) = n_0 f(v) \tag{9}$$

for two cases:

a) Maxwell Boltzmann (M.B.),

$$\frac{f(v)}{v^2} = 4\pi \left(\frac{m}{2\pi K_0 T}\right)^{3/2} \exp\left\{-\left(\frac{mv^2}{2kT}\right)\right\} \tag{10a}$$

b) a flat topped (F.T.) distribution which represents the asymptotic self-similar solution relevant to the Langdon effect,

$$\left(\frac{1}{\nu_0}\, 3\right) \quad \exp\left\{-\left(\frac{\nu}{\nu_0}\right)^5\right\}$$

This distribution can be approximately represented as:

$$\frac{f(v)}{v^2} = \frac{3}{v_0^3} \qquad v \leq v_0 \tag{10b}$$

$$= 0 \qquad v > v_0$$

Note that the distribution is a speed distribution and that v_0 is the velocity at some time when the original distribution is no longer part of the evolution. These two distributions, together with Eq. 8, can be rearranged to show that the logarithm of the emissivity as a function of frequency is given by:

$$\text{M.B.:} \quad \log(\eta_\nu) \propto -(h\nu/KT) \tag{11a}$$

$$\text{F.T.:} \quad \log(\eta_\nu) \propto \text{constant} \quad \text{for } h\nu \leq E_I + 1/2\, mv_0^2$$
$$\propto 0 \qquad \text{for } h\nu \geq E_I + 1/2\, mv_0^2 \tag{11b}$$

Thus one would expect a constant slope for the F.T. distribution with a rapid decrease above a certain photon energy.

II. Experimental Method

A schematic of our experiment is shown in Figure 2. In essence, we measured the time evolution of the K-shell free bound spectrum that is emitted from the coronal plasma produced by a laser-irradiated aluminum disk. We utilized the single-beam Vulcan Laser at the Rutherford-Appleton Laboratories' Central Laser Facility. Laser output parameters were nominally $\sim$800 psec pulsewidth and λ_L = 0.53 μm wavelength. The laser was focussed to a minimum spot size of $\sim$50 μm diameter which produced intensities of $I_L \sim 0.5\text{-}1.0 \times 10^{16}$ W/cm^2, the variation owing to fluctuations in laser energy output (15-30 joules). The surface of the disk was oriented perpendicular to

the direction of the laser beam. A streaked x-ray spectrograph[8], which utilized a *RAP* crystal to diffract photons into an x-ray streak camera, was positioned at 90° relative to the incident laser beam. The geometry of the spectrograph plus the limited width of the streak-camera cathode (2 cm) restricted the energy coverage to the interval 2.2 keV-3.0 keV. This interval is adjustable in terms of centroid energy but not width. For more details concerning this instrument see reference 8. This energy interval was chosen to cover the Al XIII recombination edge and higher energies. The relative efficiency of the streak camera spectrograph was obtained by normalizing to a spectrum obtained simultaneously using a conventional time-integrated spectrograph. This normalization requires the integration of the time-resolved spectrum over the measured time interval (0 to 2.5 nsec).

To ensure that the spectrograph measured only x-rays emitted from the coronal plasma, the viewing region is restricted using a mask located 25 μm or more from the disk surface; as can be seen in Figure 2. The mask is made of Ti that is 25 μm thick and therefore opaque to any x-rays of interest. The mask is placed adjacent to the target (at ~50 μm from the edge of the disk). Density profiles obtained by interferometry[9] for laser-produced plasmas generated by similar conditions indicate that with the plasma masked as indicated, we are only looking at the corona.

In Figure 2 is a picture of the time-resolved spectrum. The signal/noise ratio is sufficient to observe the free-bound emission spectrum for a time interval ~2 nsec. This interval of emission far exceeds the laser pulselength (FWHM).

Figure 3 represents a 2-D image of the film produced by a storage of film density vs. position on a VAX 11/780 computer system. In Figures 4a-d and 5a-c we show spectra corresponding to different time intervals corresponding to when the laser is on and then off. As marked in Figure 4 these spectra are obtained by averaging the energy spectrum for a given time interval.

Figure 6 represents a typical spectrum obtained with a time-integrated spectrograph utilized in this same set of measurements. The illustrated spectral regions have similar shape in both time-resolved and time-integrated spectrographs only if the time resolved data is integrated over the entire observation interval. Otherwise the spectra exhibit marked differences for a given time interval. If you wish to determine electron temperature in a laser-produced plasma, this phenomenon should illustrate the futility of using the time-integrated spectrum of freebound emission.

Discussion

The spectra shown in Figure 4a-d represent the emission observed during the time intervals 200-400 psec, 400-600 psec, 800-1000 psec, and 1200-1400 psec, respectively. These times roughly correspond to those during which the laser is heating the plasma (recall the pulselength is

$\sim$ 800 psec FWHM). The spectra produced during the first three time intervals are nearly identical except for relative emission levels, the 400-600 psec interval being the most intense. These spectra are characterized by nearly constant intensity emission from approximately 2.2 to 2.9 keV. The rolloff in intensity above 2.9 keV is an effect due to the finite width of the streak camera cathode. On Figure 4b we have drawn the spectral shape which would be expected from a 1 keV Maxwellian. The fact that the observed spectrum is much flatter than expected for the Maxwellian indicates that, either KT is much higher ($KT \geq 6$ keV would appear flat over this narrow energy interval) or the spectrum is non-Maxwellian. The spectrum does not drop rapidly for energies larger than the threshold energy. This may be due to an electron distribution f(v) which is neither constant nor Maxwellian. The 1200-1400 psec interval spectrum begins to illustrate some slope towards lower intensity at higher photon energies. This should indicate some cooling of the plasma late in the laser pulse.

Figure 5a-c illustrates a method to obtain the time rate of change (or cooling rate) of the plasma temperature, provided the laser is off. Presuming that late in the lifetime of the plasma we can characterize f(v) as a Maxwellian, then it should be valid to use the slope of the freebound emission to determine electron temperature. Under these circumstances it is easy to show that the plasma cools from $KT \sim 210$ eV in the 1600-1800 psec interval down to $KT \sim 90$ eV in the 2200-2400 psec time segment.

There appears a "hump" in all three spectra represented in Figs. 5a-c which is centered at $h\nu \sim 2.9$ keV. This effect is instrumental, although we have not isolated a cause. If it is real, it represents contributions from electrons having some net velocity relative to the plasma as a whole. This phenomenon would produce a positive shift in the spectrum corresponding to the equivalent velocity of the plasma center of mass relative to the nonisotropic electron source. A net velocity of free electrons relative to the capturing ions of $v_e \sim 1.5 \times 10^9$ cm/sec would be sufficient to shift the recombination spectrum by $\sim$600 eV. As another possible explanation, we may observing an isotropic but non-thermal distribution which peaks around $\sim$600 eV (i.e., nearly monoenergetic). Further experiments with a better characterized detector will be needed to study this "bump".

Conclusions

We observe a flat-topped spectrum only when the laser is on which is indicative of either a non-Maxwellian $f(v)$ or a $KT >> 1$ keV. Spectral coverage over a larger energy range is needed to resolve this ambiguity. This will require re-design of our time resolved instrument to lower its dispersion. As an aside we note that we can easily measure the cooling rate of the plasma after the laser is off by measuring the time rate of change in the free-bound slope.

References

1. A. B. Langdon, Phys. Rev. lett. 44, 575 (1980).

2. J. Dawson, "A Radiation from Plasmas", Advances in Plasma Physics, Vol. 1, edited by A. Simon and W. Thompson (Interscience, N.Y., 1981).

3. J. Dawson and C. Oberman, Phys. Fluids 5, 517 (1962) and 6, 394 (1963).

4. V. L. Ginsburg, Propagation of Electromagnetic Waves in Plasmas, (Pergramon, N.Y., 1964) Chs. 4 and 6.

5. N. G. Denisov, Sov. Phys. - JETP 4, 544 (1957); A. D. Piliya, Sov. Phys. - Tech. Phys. 11, 609 (1966); J. P. Friedberg, R. W. Mitchell, R. L. Morse and L. I. Rudsinski, Phys. Rev. Lett. 28, 795 (1972); T. Speziale and P. Catto, Phys. Fluids 20, 990 (1977).

6. R. Faehl and W. L. Kruer, Phys. Fluids 20, 55 (1977); W. Manheimer, Phys. Fluids 20, 265 (1977); W. Manheimer, D. Colombant, and B. Ripin, Phys. Rev. Lett 38, 1135 (1977); and W. Manheimer and D. Colombant, Phys. Fluids 21, 1818 (1978).

7. D. G. Colombant and W. M. Manheimer, Phys. Fluids 23, 2512 (1980).

8. C. L. S. Lewis, M. J. Lamb, J. D. Kilkenny, S. Veats, M. H. Key, described in Annual Report to the Laser Facility Committee 1980, Science Research Council Central Laser Facility, Rutherford Laboratory, Report #RL-80-026, Ch. 6. (Rutherford Laboratory, Chilton, Didcot, Oxfordshire, OX11 0QX, England).

9. O. Willi, Rutherford Laboratory, private communication.

Figure Captions

1. Non-Maxwellian electron distribution function produced by inverse bremsstrahlung absorption when $Z\ (v_0/v_{te})^2 > 1$. The two curves show distibutions when $Z\ (v_0/v_{te})^2 < 1$ (Maxwellian) and $Z\ (v_0/v_{te})^2 = 6$.

2. Schematic of Experiment.

3. 2-D representation of digitized film data. Shaded region illustrates time interval that can be arbitrarily set to take a snapshot of x-ray spectrum.

4.a-d Snapshot of Al K x-ray spectrum obtained over noted time intervals which correspond to when laser is heating plasma.

5.a-c Snapshots of Al K x-ray spectrum obtained over noted time intervals which correspond to after laser heating is shut off.

6. Al K x-ray spectrum obtained with conventional time-integrating spectrograph.

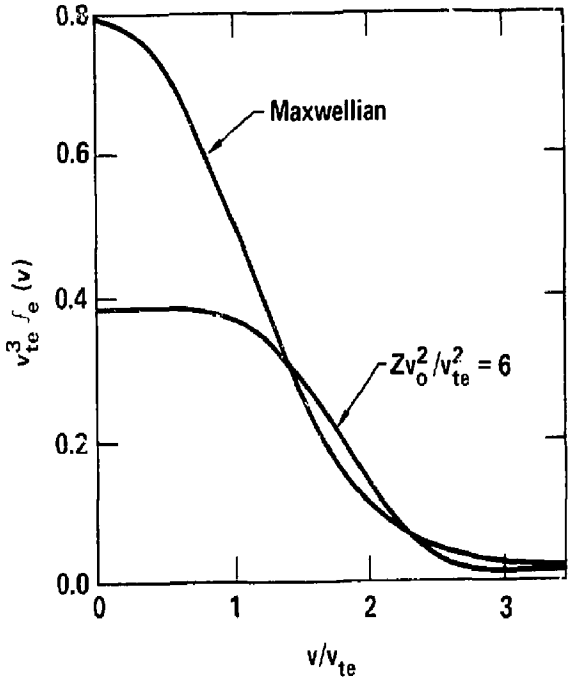

FIG. 1

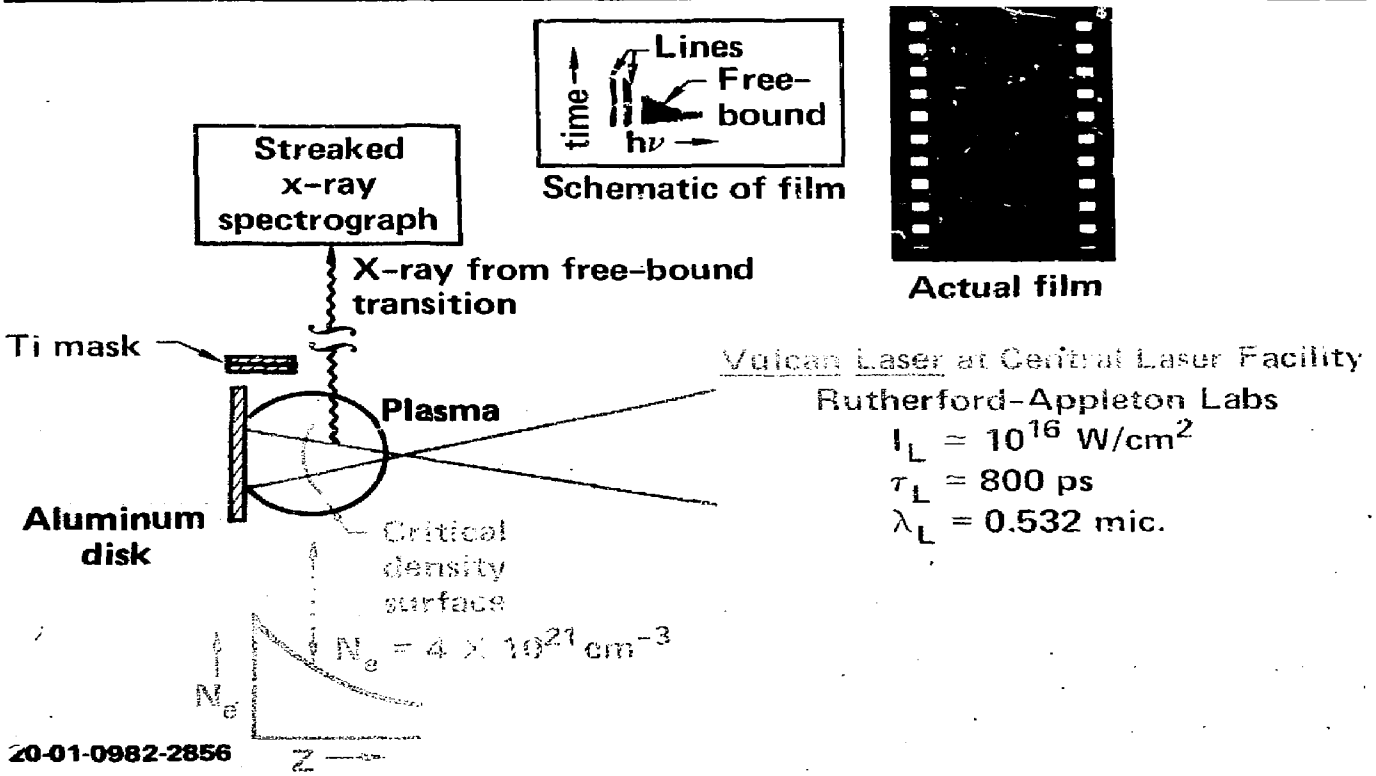
Lines
Free–
bound
time
hν
Schematic of film
Actual film
Streaked
x-ray
spectrograph
X-ray from free-bound
transition
Ti mask
Plasma
Aluminum
disk
Critical
density
surface
$N_e = 4 \times 10^{21}\ cm^{-3}$
N_e
Z
20-01-0982-2856
Vulcan Laser at Central Laser Facility
Rutherford-Appleton Labs
$I_L \simeq 10^{16}\ W/cm^2$
$\tau_L \simeq 800\ ps$
$\lambda_L = 0.532\ mic.$

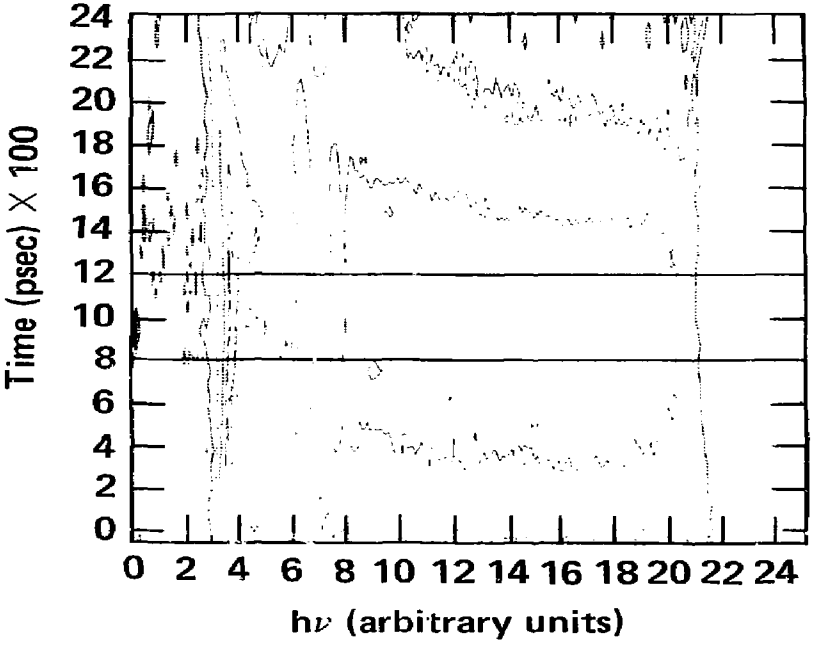
Time (psec) X 100
24
22
20
18
16
14
12
10
8
6
4
2
0
0 2 4 6 8 10 12 14 16 18 20 22 24
hν (arbitrary units)

FIG. 3

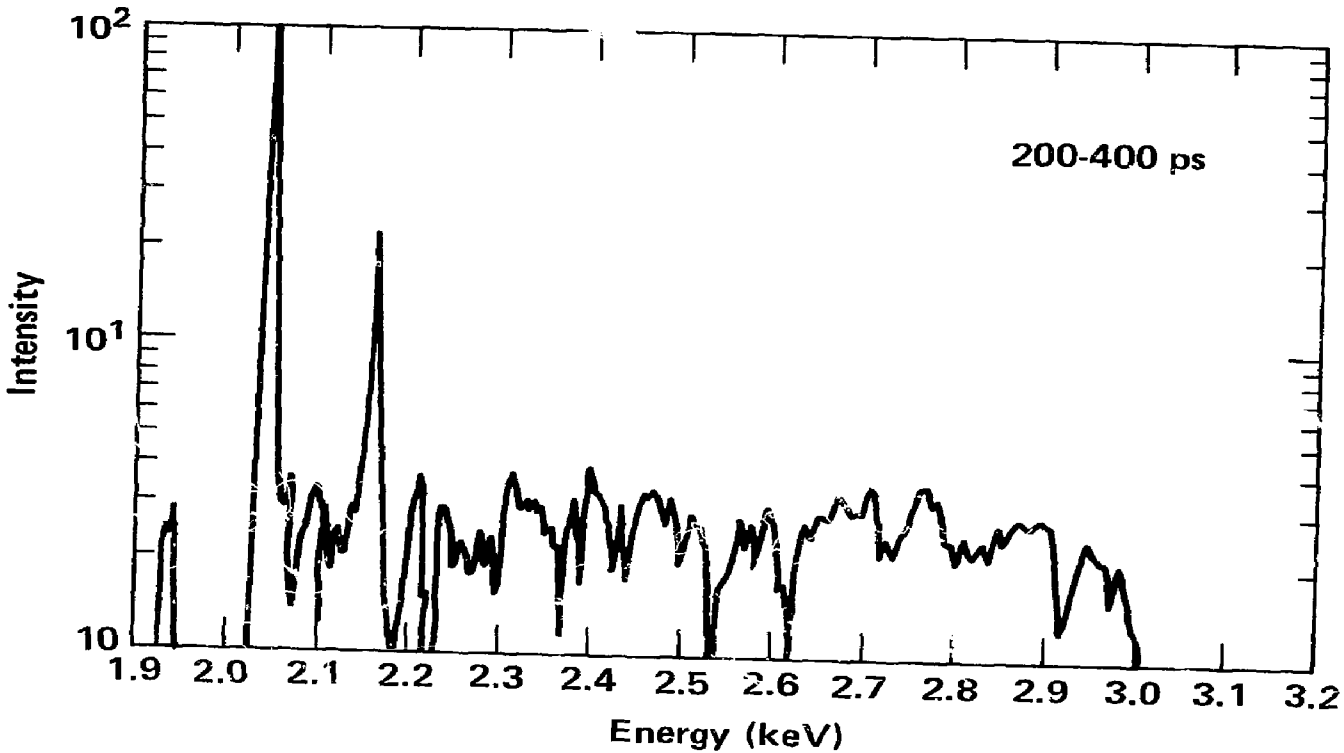
200-400 ps
Intensity
10^2
10^1
10
1.9
2.0
2.1
2.2
2.3
2.4
2.5
2.6
2.7
2.8
2.9
3.0
3.1
3.2
Energy (keV)

FIG. 4a

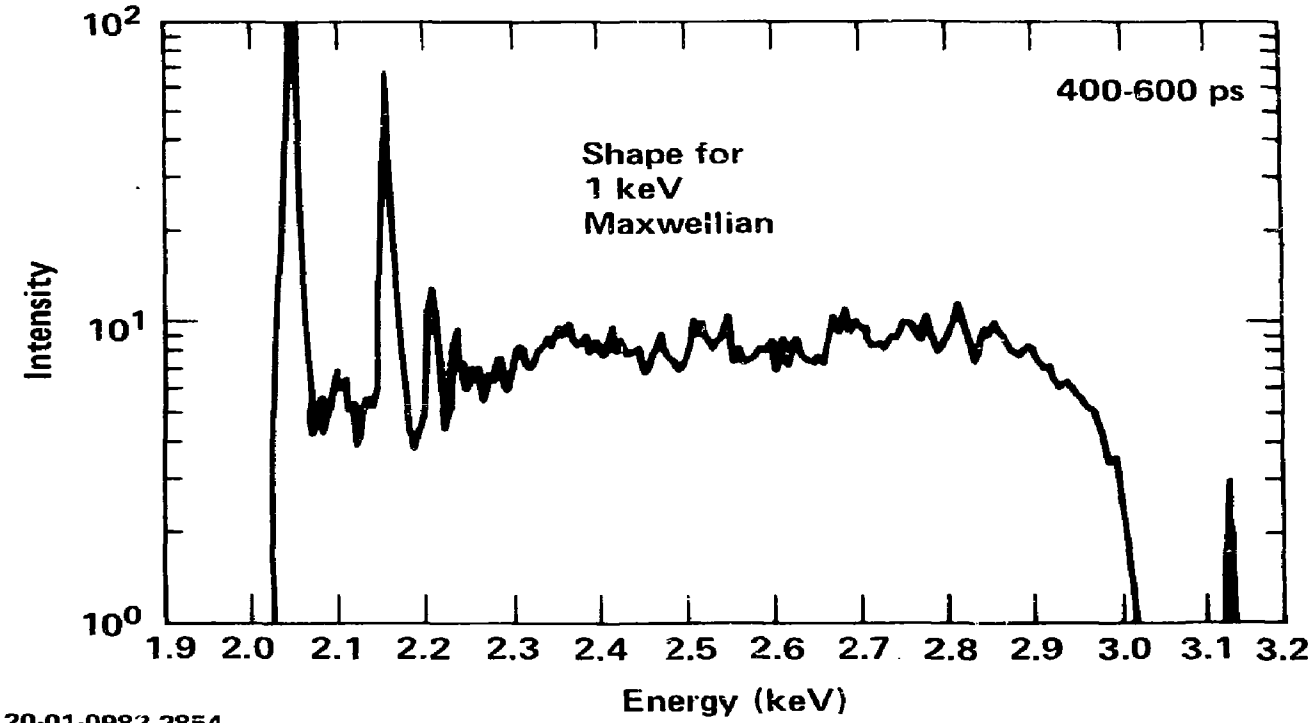
400-600 ps
Shape for
1 keV
Maxwellian
Intensity
10^2
10^1
10^0
1.9 2.0 2.1 2.2 2.3 2.4 2.5 2.6 2.7 2.8 2.9 3.0 3.1 3.2
Energy (keV)
20-01-0982-2854

FIG. 4b

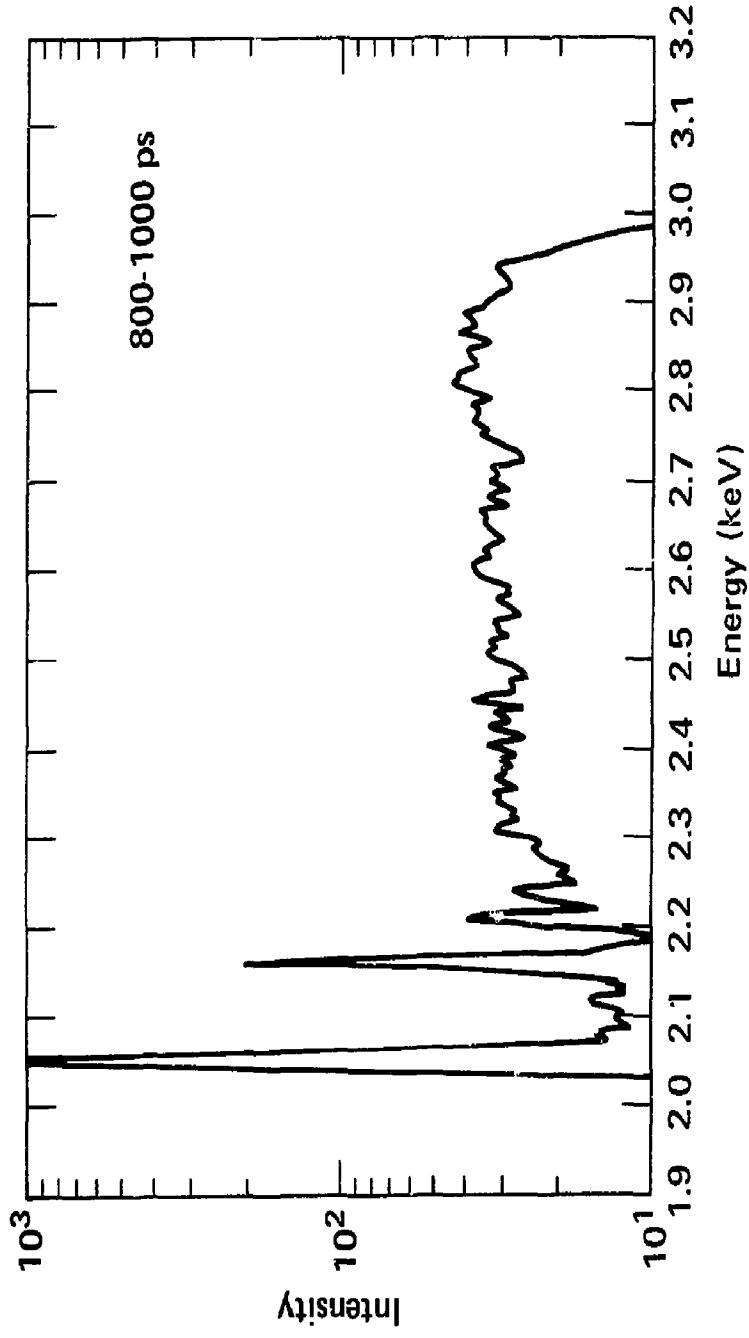
800-1000 ps
Intensity
10^3
10^2
10^1
1.9
2.0
2.1
2.2
2.3
2.4
2.5
2.6
2.7
2.8
2.9
3.0
3.1
3.2
Energy (keV)

FIG. 4c

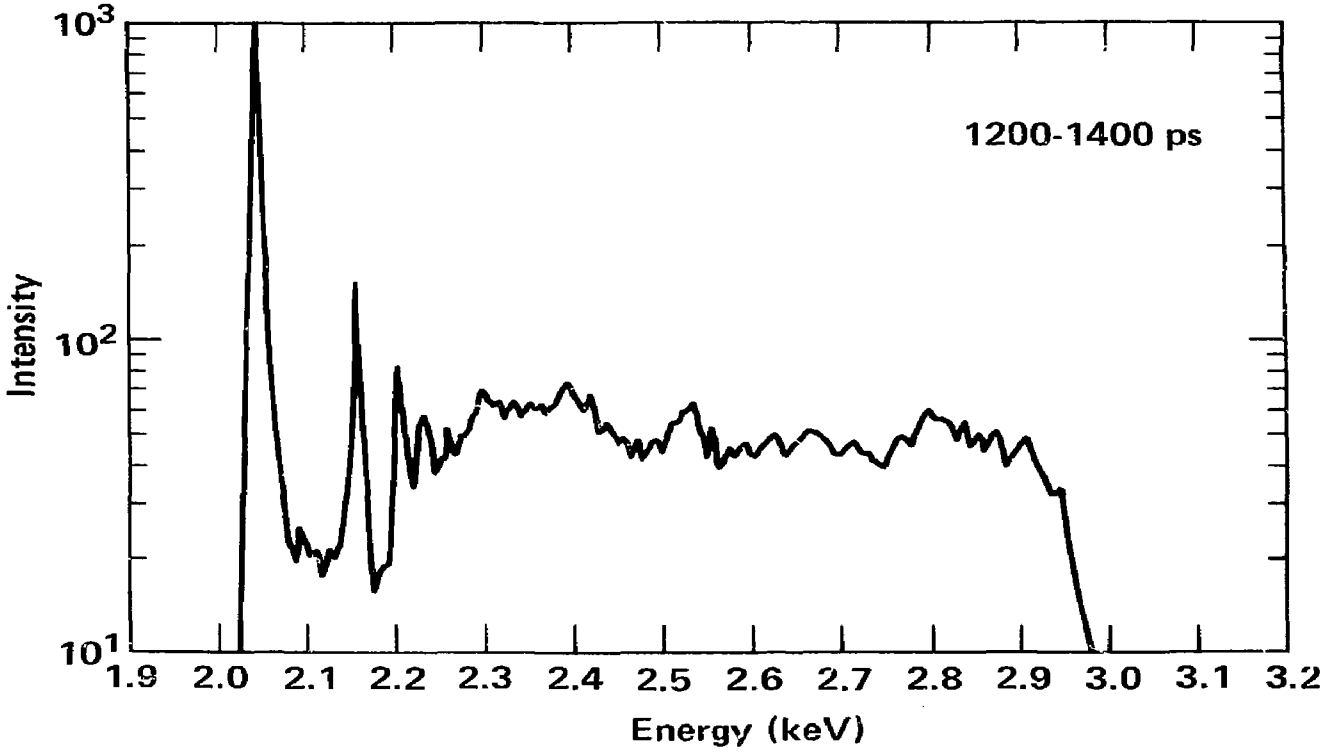
1200-1400 ps
Intensity
10^3
10^2
10^1
1.9
2.0
2.1
2.2
2.3
2.4
2.5
2.6
2.7
2.8
2.9
3.0
3.1
3.2
Energy (keV)

FIG. 4d

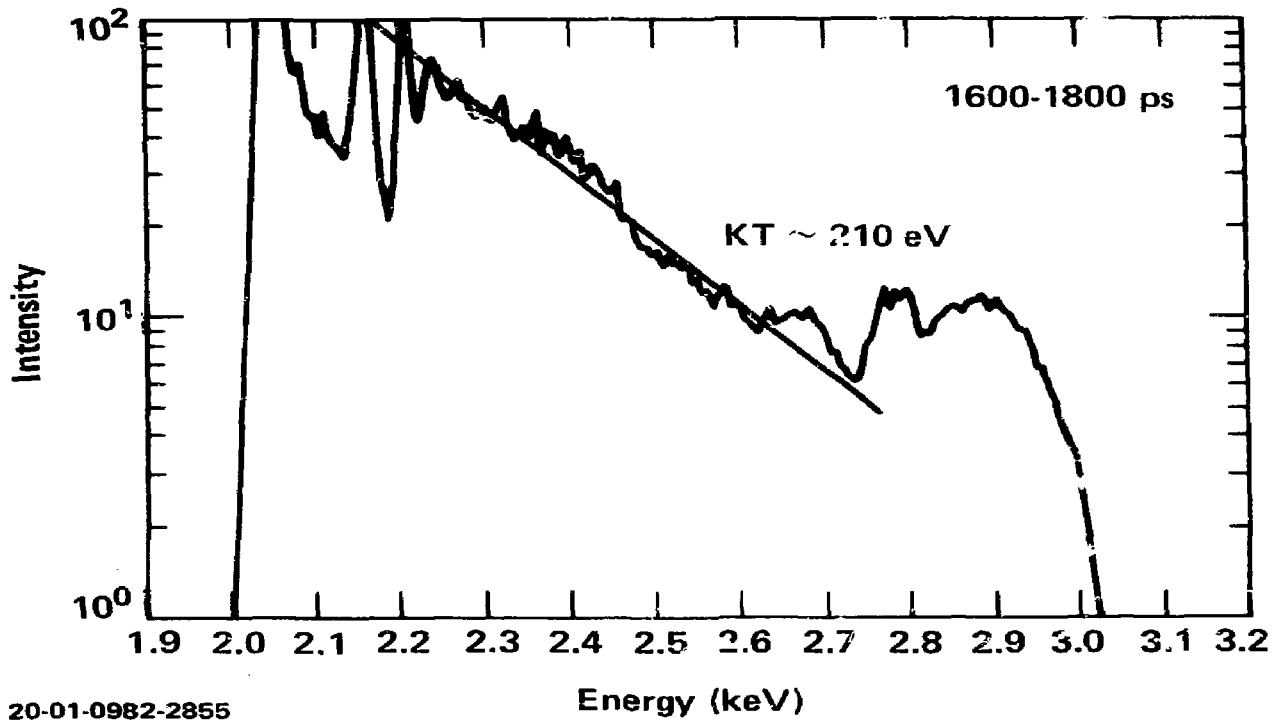
1600-1800 ps
KT ~ 210 eV
Intensity
10^2
10^1
10^0
1.9 2.0 2.1 2.2 2.3 2.4 2.5 2.6 2.7 2.8 2.9 3.0 3.1 3.2
Energy (keV)
20-01-0982-2855

FIG. 5a

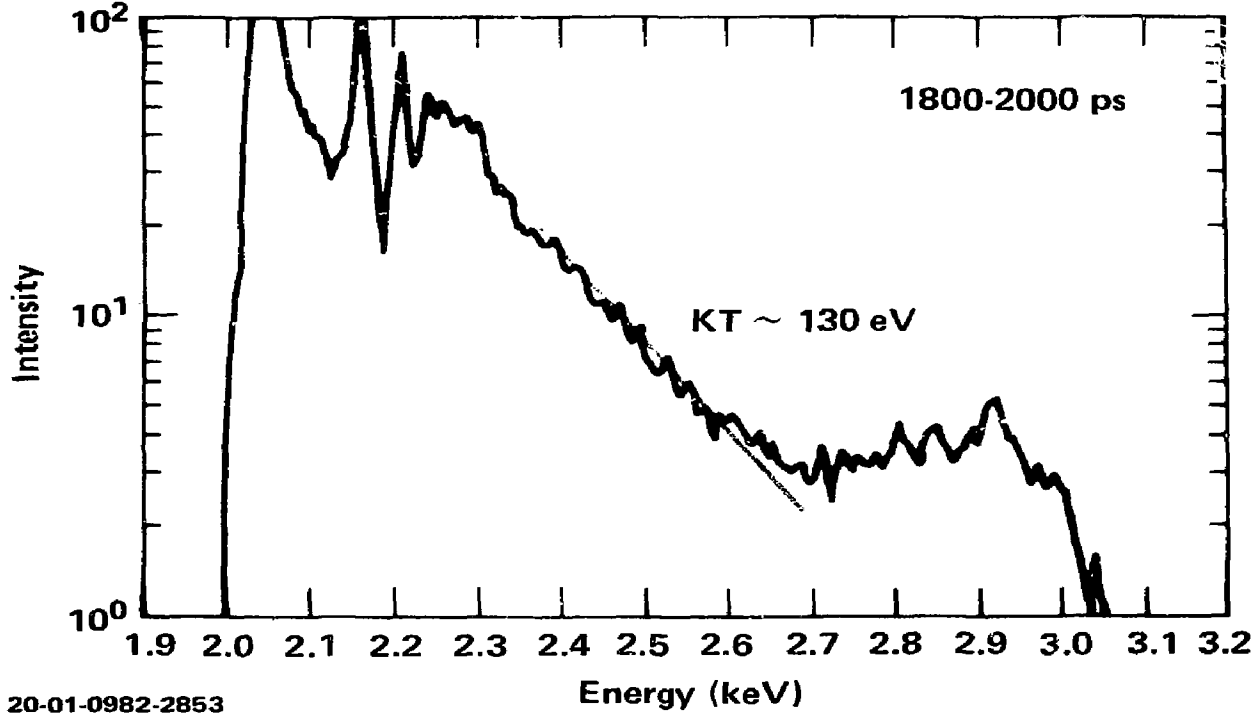
1800-2000 ps
KT ~ 130 eV
Intensity
10^2
10^1
10^0
1.9 2.0 2.1 2.2 2.3 2.4 2.5 2.6 2.7 2.8 2.9 3.0 3.1 3.2
Energy (keV)
20-01-0982-2853

FIG. 5b

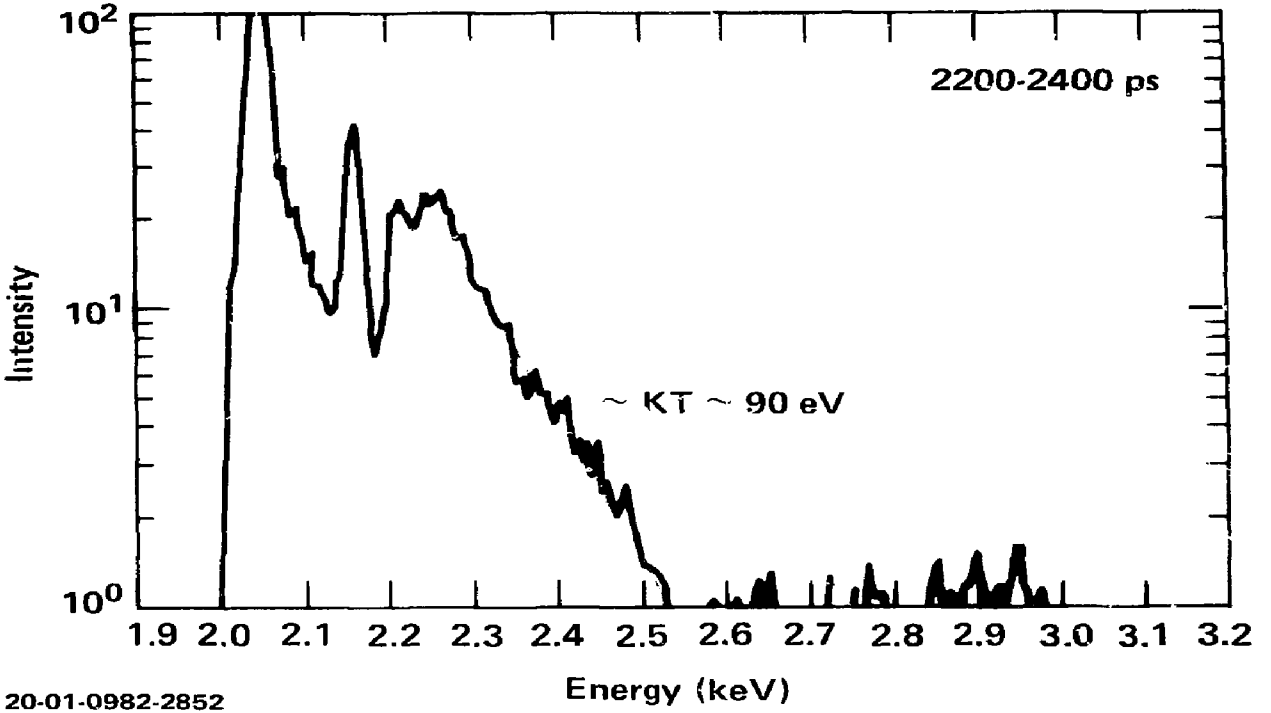
2200-2400 ps
~ KT ~ 90 eV
Intensity
10^2
10^1
10^0
1.9 2.0 2.1 2.2 2.3 2.4 2.5 2.6 2.7 2.8 2.9 3.0 3.1 3.2
Energy (keV)
20-01-0982-2852

FIG. 5c

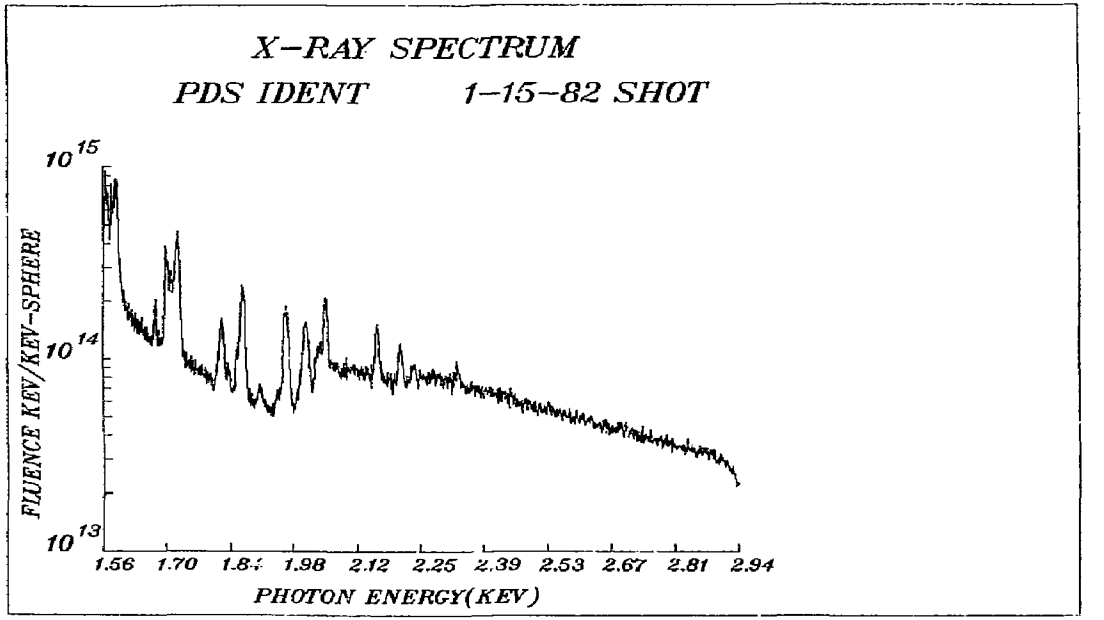
X-RAY SPECTRUM
PDS IDENT 1-15-82 SHOT
FLUENCE KEV/KEV-SPHERE
10^15
10^14
10^13
1.56 1.70 1.84 1.98 2.12 2.25 2.39 2.53 2.67 2.81 2.94
PHOTON ENERGY(KEV)

FIG. 6